*Int. J. Heat Mass Transfer.* Vol. 8, pp. 721–728. Pergamon Press 1965. Printed in Great Britain

# THE STABILITY OF THERMALLY INDUCED FLOW IN THE CORELESS INDUCTION FURNACE

**N. J. DAMASKOS and F. J. YOUNG**
Carnegie Institute of Technology, Pittsburgh, Pa., 15213, U.S.A.

(*Received* 7 *August* 1964 *and in revised form* 6 *November* 1964)

**Abstract**—The stability of the previously derived steady laminar flow of an idealized induction furnace is analysed by means of the perturbation technique commonly used for stability analyses [1]. It is shown that the minimum critical Grashof number for molten iron is 19 000 occurring for a skin depth to radius ratio of one half. Calculation then shows that the tolerable temperature gradient across a radius is very small so that stirring action under the influence of thermal buoyancy forces is generally turbulent.

## INTRODUCTION

IN A PREVIOUS paper [1] a steady laminar solution to the thermally induced flow of an induction furnace was obtained using the idealization shown in Fig. 1. Density variations in the charge, brought about by temperature differences, give rise to buoyancy forces under whose influence the fluid motion is upward near the axis and down near the walls. This mode of operation of the furnace is important only when the magnetic field is almost entirely axial so that the effect of electromagnetic stirring can be neglected. Accordingly, an infinite model was used to eliminate electromagnetic stirring forces. Rectangular rather than cylindrical coordinates were used to avoid Bessel functions for the sake of computational ease. In that analysis the velocity $V_y$, temperature $T$, and complex magnetic field $H_y$, (with exponential variation $\exp[j\omega_0 t]$ understood) were found to be

$$\frac{\mu V_g}{\rho_0 g \beta} = \frac{I^2}{4\sigma\kappa}\left[\frac{b^2 - x^2}{2} - \frac{\delta^2}{4}\left(\frac{\text{ch}\, 2b/\delta - \cos 2b/\delta}{\text{ch}\, 2b/\delta + \cos 2b/\delta} - \frac{\text{ch}\, 2x/\delta - \cos 2x/\delta}{\text{ch}\, 2b/\delta + \cos 2b/\delta}\right)\right] + (T_1 - T_L)\frac{b^2 - x^2}{2} \tag{1}$$

$$T = T_1 + \frac{I^2}{4\sigma\kappa}\left(1 - \frac{\text{ch}\, 2x/\delta + \cos 2x/\delta}{\text{ch}\, 2b/\delta + \cos 2b/\delta}\right) \tag{2}$$

$$H_y = I\frac{\text{ch}\,(1 + j)x/\delta}{\text{ch}\,(1 + j)b/\delta}, \quad j = \sqrt{-1} \tag{3}$$

$$T_L = T_1 + \frac{I^2}{4\sigma\kappa}\left[1 + 3(\delta/2b)^3 \frac{\text{sh}\, 2b/\delta - \sin 2b/\delta}{\text{ch}\, 2b/\delta + \cos 2b/\delta} - 3(\delta/2b)^2\frac{\text{ch}\, 2b/\delta - \cos 2b/\delta}{\text{ch}\, 2b/\delta + \cos 2b/\delta}\right] \tag{4}$$

where $T_1$ is the wall temperature, $\sigma$ and $\kappa$ are the electrical and thermal conductivities, and the skin depth $\delta = \sqrt{(2/\omega_0\mu_0\sigma)}$ ($\mu_0$ is the permeability). These represent solutions to the system of magnetohydrodynamic equations

$$\rho_0^*\left[\frac{\partial \mathbf{V}^*}{\partial t} + (\mathbf{V}^* \cdot \nabla)\,\mathbf{V}^*\right] = -\nabla p^* + \mu\nabla^2\,\mathbf{V}^* + \mu_0(\nabla \times \mathbf{H}^*) \times \mathbf{H}^* + \rho^*\mathbf{g} \tag{5}$$

where $\rho^* = \rho_0[1 - \beta(T^* - T_0)]$

$$\nabla \cdot \mathbf{V}^* = 0 \tag{6}$$

$$\rho_0^*\, C_v\left[\frac{\partial T^*}{\partial t} + (\mathbf{V}^* \cdot \nabla) T^*\right] = \kappa\nabla^2\, T^* + \frac{(\nabla \times \mathbf{H}^*)^2}{\sigma} \tag{7}$$

$$\nabla^2\mathbf{H}^* + \mu_0\sigma\,\nabla \times (\mathbf{V}^* \times \mathbf{H}^*) = \mu_0\sigma\frac{\partial \mathbf{H}^*}{\partial t} \tag{8}$$

$$\nabla \cdot \mathbf{H}^* = 0 \tag{9}$$

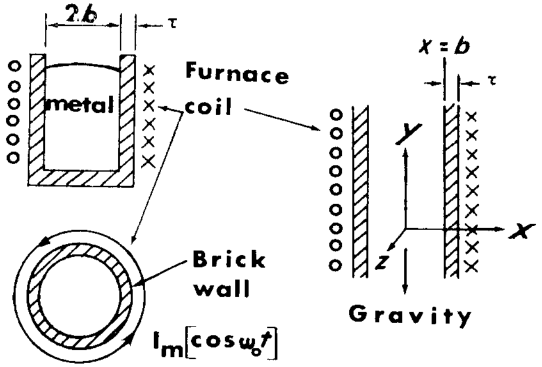


FIG. 1. Geometry of idealized model for thermally induced flow; $I$ = linear current density of coil in A/unit, $y$ = dimension, $\omega_0$ = frequency in radians/s, $b$ = furnace radius in meters, $t$ = time in seconds.

after taking time averages of the equations over one cycle in time and assuming the fluid is incompressible. Note that unstarred quantities are time averages of the corresponding time dependent starred quantities. The assumption employed in this process is that the mechanical and thermal time constants are long compared with the electrical period of excitation so that there is only a steady velocity, pressure and temperature response to the d.c. component of the forcing functions. Quantities not defined so far are: $T_0$, a constant mean temperature from which temperature variations are measured; $\rho_0$, the mean density corresponding to $T_0$; $\mu$, the dynamic viscosity; $\beta$, the coefficient of volume expansion; $g$ the gravitational acceleration; $C_v$, the specific heat at constant volume; and $P$, the pressure.

The object of this analysis is to determine the range of parameters over which the thermally driven flow just described is stable. The problem arises since flows originating from free convection are known to be easily disturbed. The approach is very similar to the work of Gershuni and Zhukhovitskii [2] who have studied the stability of stationary convective flow of a liquid conductor between heated vertical plates in the presence of a d.c. magnetic field. For the purpose of checking the equations derived here, their terminology is followed closely, even though this problem deals with a.c. fields.

Basically, the approach is to perturb the steady laminar solution assuming changes in the fields of small amplitude. The perturbed quantities are given an exponential variation with time and are made space periodic with respect to the coordinate variables for which the flow goes to infinity or does not vary. For the model under consideration the variations take the form $f(x) \exp[j(\omega t - \kappa y)]$ where $f(x)$ determines the profile; the reciprocal wave number, $1/\kappa$, the size of the cell; and the frequency, $\omega$, the stability of the flow. This form gives rise to plane perturbations, although a more detailed analysis would specify a wave number for the $z$-direction, corresponding to cell structure in the azimuthal direction of cylindrical coordinates.

The classic example illustrating the cell structure that develops is the Bénard problem of the instability of a layer of fluid heated from below [3, 4]. Here, as the buoyancy forces increase under the influence of an adverse temperature gradient, a critical gradient is reached at which these forces exceed the viscous forces. The fluid then breaks from the stable or motionless state into instability which manifests itself as steady thermal convection within a cellular pattern that is periodic in all horizontal directions. The critical gradient is expressed as a critical Grashof number which is a measure of the ratio of inertial forces induced by convection to the viscous forces or as the product of the Grashof and Prandtl numbers called the Rayleigh number.

Instability, however, need not set in as steady convection as in the Bénard problem (corresponding to $\omega = 0$) but may appear as traveling perturbations. This is determined by the nature of the frequency $\omega$ for which solutions to the perturbation equations exist.

For a given flow to be stable any disturbance must decay with time, indicating that $\mathrm{Im}(\omega) > 0$ where Im means imaginary part of. On the other hand, the flow is unstable and the disturbance increases with time when $\mathrm{Im}(\omega) < 0$. Thus, one is interested in solving for the neutral perturbation state defined by the condition $\mathrm{Im}(\omega) = 0$ in which $\omega$ is a real quantity. When instability in the form of stationary convection does in fact arise, the solution $\omega = 0$ results but may not be assumed *a priori*.

In brief, the steps in the analysis are as follows. First, the perturbations are given an exponential form and are substituted into the perturbation equations. The result is an eigenvalue problem for which solutions in $\omega$ and $\kappa$ are sought as some physical parameter (the Grashof number in this case) is varied. When approximate functions are used, a homogeneous system of equations results, and the eigenvalue problem arises by the requirement that the system determinant must vanish for solutions to exist. The remainder of the procedure is to equate to zero the real and imaginary parts of the system determinant (considering $\omega$ a real quantity), eliminate $\omega$ from this pair of equations, and plot the neutral curve in the $G$–$K$ plane (where $G$ = Grashof number and $K$ = wavenumber). The stability analysis follows this procedure.

## PERTURBATION EQUATIONS

Adding the small perturbation quantities $\mathbf{v}^*$, $\theta^*$, $p^*$, and $\mathbf{h}^*$ to the stationary quantities $\mathbf{V}$, $T$, $P$, and $\mathbf{H}^*$ developed in reference 1, the quantities $\mathbf{V} + \mathbf{v}^*$, $T + \theta^*$, $P + p^*$, and $\mathbf{H}^* + \mathbf{h}^*$ must satisfy equations (5) through (9). Neglecting products of small quantities and recalling that the stationary solution already satisfies these equations, one obtains for the perturbation equations

$$\rho_0\left(\frac{\partial \mathbf{v}^*}{\partial t} + \mathbf{v}^* \cdot \nabla \mathbf{V} + \mathbf{V} \cdot \nabla \mathbf{v}^*\right) = -\nabla p^* + \mu\nabla^2 \mathbf{v}^* - \rho_0 \beta\theta^* \mathbf{g} - \mu_0 \nabla \mathbf{H}^* \cdot \mathbf{h}^* + \mu_0 \mathbf{H}^* \cdot \nabla \mathbf{h}^* + \mu_0 \mathbf{h}^* \cdot \nabla \mathbf{H}^* \tag{10}$$

$$\rho_0 C_v \left(\frac{\partial \theta^*}{\partial t} + \mathbf{v}^* \cdot \nabla T + \mathbf{V} \cdot \nabla\theta^*\right) = \kappa\nabla^2 \theta + \frac{2}{\sigma}[(\nabla\times \mathbf{H}^*)\cdot(\nabla\times \mathbf{h}^*)],$$

$$\nabla \cdot \mathbf{v}^* = 0, \quad \text{and} \quad \nabla \cdot \mathbf{h}^* = 0 \tag{11}$$

$$\mu_0\sigma\left[\frac{\partial \mathbf{h}^*}{\partial t} + \nabla\times(\mathbf{h}^* \times \mathbf{V}) + \nabla\times(\mathbf{H}^* \times \mathbf{v}^*)\right] = \nabla^2 \mathbf{h}^* \tag{12}$$

Now the time variation of the perturbation terms is $\exp[j\omega t]$. The terms involving the magnetic fields in the right side of equation (10) are neglected in this analysis. These terms represent a retarding body force exerted upon the fluid when it flows in the radial direction. The force arises from the interaction of the applied axial magnetic field with the azimuthal current induced by the radial flow of the liquid metal. When the force is averaged in time, it varies as $\exp[j\omega t]$. This force increases the stability of the stationary flow [2]. However, in the coreless induction furnace this force is weakened by the skin effect which greatly lowers the amplitude of the applied magnetic field in regions located more than one skin depth away from the containing vessel wall. The dropping of the induced body force is also consistent with the magnetic Reynolds number encountered in most furnaces. Using a value of 0·46 m as the characteristic size and letting the velocity be 10 cm/s (reasonable for stirring due to buoyant forces) [11] yields a magnetic Reynolds number of 0·04. Hence our solution neglects the stabilizing body force and applies when $R_m \ll 1$ and $b' > 2$. Equations (10) and (11) are then written more simply as

$$\rho_0\left(\frac{\partial \mathbf{v}^*}{\partial t} + \mathbf{v}^* \cdot \nabla \mathbf{V} + \mathbf{V} \cdot \nabla \mathbf{v}^*\right) = -\nabla p^* + \mu\nabla^2 \mathbf{v}^* - \rho_0 \beta\, \theta^* \mathbf{g} \tag{13}$$

$$\rho_0 C_v \left(\frac{\partial \theta^*}{\partial t} + \mathbf{v}^* \cdot \nabla T + \mathbf{V} \cdot \nabla\theta^*\right) = \kappa\nabla^2 \theta^* \tag{14}$$

and no longer depend on the magnetic field. In other words, flow induced magnetic fields are considered to be small compared to the applied field $H_y^*$. The curl of (13) eliminates the pressure gradient and yields

$$\rho_0 \nabla\times\left(\frac{\partial \mathbf{v}^*}{\partial t} + \mathbf{v}^* \cdot \nabla \mathbf{V} + \mathbf{V} \cdot \nabla \mathbf{v}^*\right) = \mu\nabla\times\nabla^2 \mathbf{v}^* - \rho_0 \beta \nabla\times\theta^* \mathbf{g} \tag{15}$$

which may be solved together with (14) for the velocity and temperature perturbations.

When a plane perturbation is assumed with no motion in the $z$ direction, the quantities depend on $x$, $y$, and $t$ and vary as $f(x)\exp[j(\omega t + \kappa y)]$. Choosing a stream function $\psi^*$ the velocity components are

$$v_x^* = -\frac{\partial}{\partial y}\left[\psi(x)\exp[j(\omega t + \kappa y)]\right] \tag{16}$$

$$v_y^* = \frac{\partial}{\partial x}\left[\psi(x)\exp[j(\omega t + \kappa y)]\right] \tag{17}$$

and the temperature perturbation is

$$\theta^* = \theta(x)\exp[j(\omega t + \kappa y)] \quad (18)$$

Recalling that $\mathbf{V} = V_y(x)\,\mathbf{j}$ and $T = T(x)$ and noting that $\partial/\partial x = '$, $\partial/\partial y = jk$ and $\partial/\partial t = j\omega$ equations (14) and (15) become, upon substituting (16) to (18).

$$\rho_0\,[j\omega(\psi^{\mathrm{II}} - \kappa^2\psi) - j\,\kappa V_y''\,\psi + j\,\kappa V_y\,\psi^{\mathrm{II}} - j\,\kappa^3 V_y\,\psi] = \mu(\psi^{\mathrm{IV}} - 2\kappa^2\psi^{\mathrm{II}} + \kappa^4\psi) + \beta g\theta' \quad (19)$$

$$\rho_0\,C_v\,(j\omega\theta + j\kappa\,V_y\,\theta - j\kappa\,T'\,\psi) = \kappa(\theta'' - \kappa^2\theta) \quad (20)$$

For ease of solution the equations are put into dimensionless form. Choosing the "radius" $b$ as a measure of distance, $\nu/b$ (where $\nu = \mu/\rho_0$ is the kinematic viscosity) as a measure of velocity, $\nu/b^2$ as a measure of frequency, and the maximum difference $Q_1 = I^2/4\sigma\kappa$ as a measure of temperature, one defines the dimensionless variables

$$\mathbf{X} = x/b, \quad \boldsymbol{\psi} = \psi/\nu, \quad \mathbf{K} = \kappa b, \quad \boldsymbol{\Omega} = \omega b^2/\nu,$$
$$\mathbf{V} = V_y b/\nu, \quad \boldsymbol{\Theta} = \theta/Q_1, \quad \mathrm{t} = (T - T_1)/Q_1.$$

Defining the Prandtl number $P_r = \mu C_v/k$, the Grashof number $G = \beta g b^3 Q_1/\nu^2$, the diameter to skin depth ratio $b' = 2b/\delta$, displaying $\mathbf{V}$ and t [given by equations (1) and (2)], the dimensionless perturbation equations are

$$\boldsymbol{\psi}^{\mathrm{IV}} - 2\mathbf{K}^2\boldsymbol{\psi}^{\mathrm{II}} + \mathbf{K}^4\boldsymbol{\psi} - j\,\boldsymbol{\Omega}\,(\boldsymbol{\psi}^{\mathrm{II}} - \mathbf{K}^2\boldsymbol{\psi}) - j\,\mathbf{K}\,[(\boldsymbol{\psi}^{\mathrm{II}} - \mathbf{K}^2\boldsymbol{\psi})\mathbf{V} - \boldsymbol{\psi}\,\mathbf{V}''] + G\,\boldsymbol{\Theta}' = 0 \quad (21)$$

$$(\boldsymbol{\Theta}'' - \mathbf{K}^2\boldsymbol{\Theta}) - j\,\boldsymbol{\Omega}\,P_r\,\boldsymbol{\Theta} - j\,\mathbf{K}\,P_r\,\mathbf{V}\,\boldsymbol{\Theta} + j\,\mathbf{K}\,P_r\,\mathrm{t}'\,\boldsymbol{\psi} = 0 \quad (22)$$

where

$$\mathrm{t} = 1 - \frac{\mathrm{ch}\,b'\mathbf{X} + \cos b'\mathbf{X}}{\mathrm{ch}\,b' + \cos b'}$$

$$\mathbf{V} = G\left\{\frac{(1-\mathbf{X}^2)}{2}\left[1 - \frac{(T_L - T_1)}{Q_1}\right] - \frac{1}{b'^2}\left(\frac{\mathrm{ch}\,b' - \cos b'}{\mathrm{ch}\,b' + \cos b'} - \frac{\mathrm{ch}\,b'\mathbf{X} - \cos b'\mathbf{X}}{\mathrm{ch}\,b' + \cos b'}\right)\right\}$$

$$\frac{T_L - T_1}{Q_1} = 1 + \frac{3}{b'^3}\,\frac{\mathrm{sh}\,b' - \sin b'}{\mathrm{ch}\,b' + \cos b'} - \frac{3}{b'^2}\,\frac{\mathrm{ch}\,b' - \cos b'}{\mathrm{ch}\,b' + \cos b'}$$

The boundary conditions are that the normal and tangential perturbed velocities and the perturbed temperature should vanish at the wall, or in terms of $\psi$ and $\Theta$

$$\boldsymbol{\psi}(\pm 1) = \boldsymbol{\psi}'(\pm 1) = \boldsymbol{\Theta}(\pm 1) = 0 \quad (23)$$

## USE OF THE GALERKIN METHOD

The solution of the eigenvalue problem, defined by equations (21) and (22) and their boundary conditions, is carried out by the Galerkin method whose application to this problem is now described.

The basic idea of the method consists in approximating the solution to the differential equation by selecting a linear combination of approximate functions that satisfy the boundary conditions. These are linearly independent and represent the first $i$ functions of some system of functions chosen from a complete set in the given region. Examples of such sets are the trigonometric functions and powers of the independent variables.

Denoting the approximations to the stream function and temperature perturbations as $\tilde{\psi}$ and $\tilde{\Theta}$ and choosing the first $i$ functions $\psi_i$ and $\Theta_i$ from an appropriate complete set, such that the $\psi_i$ and $\Theta_i$ each satisfy the boundary conditions (23), then

$$\tilde{\boldsymbol{\psi}}(\mathbf{X}) = \sum_i a_i\,\boldsymbol{\psi}_i(\mathbf{X}) \quad \text{and} \quad \tilde{\boldsymbol{\Theta}} = \sum_i b_i\,\boldsymbol{\Theta}_i(\mathbf{X}) \quad (24)$$

where the Galerkin coefficients $a_i$ and $b_i$ are to be determined. Further, defining the differential operators $L(\boldsymbol{\psi}, \boldsymbol{\Theta})$ and $M(\boldsymbol{\psi}, \boldsymbol{\Theta})$, corresponding to the left side of (21) and (22) respectively, the system of equations to be solved is

$$\int_{-1}^{1} L(\tilde{\boldsymbol{\psi}}, \tilde{\boldsymbol{\Theta}})\,\boldsymbol{\psi}_i\,\mathrm{d}\mathbf{X} = 0, \quad \int_{-1}^{1} M(\tilde{\boldsymbol{\psi}}, \tilde{\boldsymbol{\Theta}})\,\boldsymbol{\Theta}_i\,\mathrm{d}\mathbf{X} = 0 \quad (25)$$

Equation (25) is a statement that one substitutes the approximate solution into the differential equations and then requires that the weighted averages of the residuals over the desired interval should vanish [5]. The weighting functions are the approximating functions. This is also referred to as an orthogonality method falling in the same category as the least squares method [6]. Duncan [7] shows the equivalence of the two methods when a large number of approximating functions is used.

If the differential equations are homogeneous, (25) leads to a homogeneous system of algebraic equations in the unknowns $a_i$ and $b_i$. These give rise to a compatibility condition which expresses the fact that (25) has a non-trivial solution only if the determinant of the set vanishes.

As pointed out in reference 8 the method is quite similar to the Ritz method, although perfectly universal in that there is not necessarily a formal connection between the given equation and a variational problem. The accuracy of the approximation improves rapidly if, in addition to the primary boundary conditions, the approximate functions satisfy secondary boundary conditions (derivable from the differential equation). Lastly, Duncan shows that if the errors in the amplitude of the approximating functions are taken to be of first order, the Galerkin method yields errors in frequency that are of the second order. This property and the inclusion of secondary boundary conditions on temperature are used as justification for restricting the approximating functions to a single term. Since the symmetry of the problem forces $\psi$ and $\Theta$ to be only even or only odd (as is shown in the following section), the accuracy of the approximation is expected to be comparable to that of the study by Gershuni and Zhukhovitskii [2] where two terms (one even and one odd) were used to approximate a condition of asymmetry.

## SOLUTION

Recalling that $\mathbf{V}$ and $\mathbf{V}''$ are even functions and that $\mathrm{t}'$ is odd, equations (21) and (22) show that even components of $\psi$ give rise to terms of odd symmetry only in $\Theta$, and also that odd terms in $\psi$ correspond only to even terms in $\Theta$. Hence, these combinations are independent, indicating the possible existence of the two modes. The mode for which $\Theta$ is even and $\psi$ odd is called the even mode, since $v_y^*$ is also an even function of $x$. Conversely, $\Theta$ odd and $\psi$ even is the odd mode. These are illustrated, at the onset of instability, in Fig. 2, the contours representing either stream lines or lines of constant temperature.

A convenient set of complete functions for constructing the $\psi_i$ and $\Theta_i$ are the powers of $\mathbf{X}$: 1, $\mathbf{X}$, $\mathbf{X}^2$, $\mathbf{X}^3$, . . . . The boundary conditions (23) show that the trial functions $\psi_i$ must vanish together with their derivatives at $\mathbf{X} = \pm 1$. For the temperature perturbation the $\Theta_i$ must vanish at $\mathbf{X} = \pm 1$, but these functions are also made to satisfy the secondary boundary condition given by (22), $\Theta''(\pm 1) = 0$. To illustrate the computation the second trial function is included in the table below:

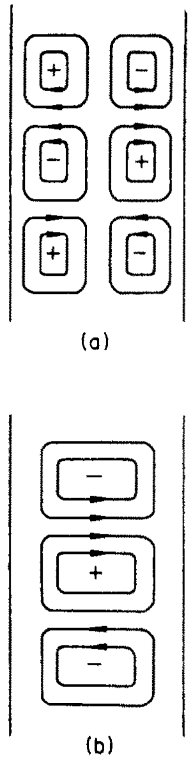

FIG. 2. Cell structure at the onset of instability. (a) The even mode cell structure which also gives the odd mode temperature cell structure. (b) The odd mode velocity cell structure which also gives the even mode temperature cell structure.

| Function | Even mode | Odd mode |
|---|---|---|
| $\psi_1$ | $\mathbf{X}(1 - \mathbf{X}^2)^2$ | $(1 - \mathbf{X}^2)^2$ |
| $\psi_2$ | $\mathbf{X}^3(1 - \mathbf{X}^2)^2$ | $\mathbf{X}^2(1 - \mathbf{X}^2)^2$ |
| $\Theta_1$ | $(1 - \mathbf{X}^2)(5 - \mathbf{X}^2)$ | $\mathbf{X}(1 - \mathbf{X}^2)(7 - 3\mathbf{X}^2)$ |
| $\Theta_2$ | $\mathbf{X}^2(1 - \mathbf{X}^2)(9 - 5\mathbf{X}^2)$ | $\mathbf{X}^3(1 - \mathbf{X}^2)(11 - 7\mathbf{X}^2)$ |

Considering only the single term approximation, $\psi = a_1\psi_1$ and $\Theta = b_1\Theta_1$, the system of equations (25) becomes

$$\left.\begin{aligned} E_{11}\,a_1 + E_{12}\,b_1 &= 0 \\ E_{21}\,a_1 + E_{22}\,b_2 &= 0 \end{aligned}\right\} \quad (26)$$

where

$$E_{11} = A_{11} + j\,\mathbf{\Omega}\,B_{11} + j\,\mathbf{K}\,G\,C_{11}$$

$$E_{12} = D_{11}$$

$$E_{21} = j\,\mathbf{K}\,P_r\,d_{11}$$

$$E_{22} = a_{11} - j\,\mathbf{\Omega}\,P_r\,b_{11} - j\,\mathbf{K}\,G\,P_r\,c_{11}$$

and where

$$A_{11} = \int_{-1}^{1} (\psi_1^{\mathrm{IV}} - 2\mathbf{K}^2\,\psi_1^{\mathrm{II}} + \mathbf{K}^4\,\psi_1)\,\psi_1\,\mathrm{d}\mathbf{X}$$

$$B_{11} = \int_{-1}^{1} (-\psi_1^{\mathrm{II}} + \mathbf{K}^2\,\psi_1)\,\psi_1\,\mathrm{d}\mathbf{X}$$

$$C_{11} = \int_{-1}^{1} [(-\psi_1^{\mathrm{II}} + \mathbf{K}^2\,\psi_1)\,\mathscr{V} + \psi_1\,\mathscr{V}'']\,\psi_1\,\mathrm{d}\mathbf{X}$$

$$D_{11} = \int_{-1}^{1} \mathbf{\Theta}_1'\,\psi_1\,\mathrm{d}\mathbf{X}$$

$$a_{11} = \int_{-1}^{1} (\mathbf{\Theta}_1'' - \mathbf{K}^2\,\mathbf{\Theta}_1)\,\mathbf{\Theta}_1\,\mathrm{d}\mathbf{X}$$

$$b_{11} = \int_{-1}^{1} \mathbf{\Theta}_1^2\,\mathrm{d}\mathbf{X}, \qquad c_{11} = \int_{-1}^{1} \mathscr{V}\mathbf{\Theta}_1^2\,\mathrm{d}\mathbf{X},$$

$$d_{11} = \int_{-1}^{1} {}'\,\psi_1\,\mathbf{\Theta}_1\,\mathrm{d}\mathbf{X}$$

and $\qquad \mathscr{V} = \mathbf{V}/G$

The script velocity, $\mathscr{V}$, has been introduced so as to make the Grashof number apparent. Dividing out the Prandtl number the system determinant is

$$\begin{vmatrix} A_{11} + j\,\mathbf{\Omega}\,B_{11} + j\,\mathbf{K}\,G\,C_{11} & G\,D_{11} \\ j\,\mathbf{K}\,d_{11} & \dfrac{a_{11}}{P_r} - j\,\mathbf{\Omega}\,b_{11} - j\,\mathbf{K}\,G\,c_{11} \end{vmatrix} = 0 \quad (27)$$

Equation (27) determines the characteristic frequencies, $\omega$, of the perturbation.

For the neutral perturbation state $\mathrm{Im}(\Omega) = 0$ and $\Omega$ is considered a real quantity. Expanding (27) and equating the real and imaginary parts to zero yields the pair of equations

$$\frac{A_{11}\,a_{11}}{P_r} + (\mathbf{\Omega}\,B_{11} + \mathbf{K}\,G\,C_{11})(\mathbf{\Omega}\,b_{11} + K\,G\,c_{11}) = 0 \quad (28)$$

$$-A_{11}\,(\mathbf{\Omega}\,b_{11} + \mathbf{K}\,G\,c_{11}) + \frac{a_{11}}{P_r}(\mathbf{\Omega}\,B_{11} + \mathbf{K}\,G\,C_{11}) - \mathbf{K}\,G\,d_{11}\,D_{11} = 0 \quad (29)$$

Since $\Omega$ is not a factor of either equation, $\Omega = 0$ is not a permissible solution. This shows that instability in the form of steady thermal convection cannot arise in the problem formulated.

Solving (29) for $\Omega$ one obtains

$$\Omega = \frac{\mathbf{K}\,G(d_{11}\,D_{11} + A_{11}\,c_{11} - (a_{11}/P_r)\,C_{11})}{-A_{11}\,b_{11} + (a_{11}/P_r)\,B_{11}} = \mathbf{K}\,G\,F(b', \mathbf{K}, P_r) \quad (30)$$

which when substituted into (28) yields the neutral curve relation in the $G$–$\mathbf{K}$ plane

$$G = \frac{1}{\mathbf{K}}\sqrt{\left(\frac{-A_{11}\,a_{11}/P_r}{(B_{11}\,F + C_{11})\,(b_{11}\,F + c_{11})}\right)} \quad (31)$$

The neutral curve relation (31) is a function of $\mathbf{K}$, $b'$ and $P_r$. Since the Prandtl number is constant for a given liquid metal one may plot neutral curves of $G$ vs $\mathbf{K}$ for each value of $b'$. The minimum value of $G$ for each curve is plotted in turn versus $b'$ and yields the desired critical curve which gives the Grashof number above which instability sets in for each value of $b'$.

## RESULTS AND CONCLUSIONS

Using equation (31) neutral stability curves of $G$ vs $\mathbf{K}$ were plotted as $b'$ was varied. The computation of the integrals $C_{11}$ and $c_{11}$ was performed numerically using Simpson's rule and 160 intervals over the normalized "radius". It was felt that this approach is less subject to error than the many integrations by parts required because of products of $\mathbf{X}^{10}$ with hyperbolic and circular functions.

It was found that symmetrical or even perturbations do not lead to instability, but that odd perturbations do. This is also true in ordinary hydrodynamics where a symmetrical stationary flow in the $y$ direction is stable for symmetrical and unstable for antisymmetrical disturbances [9]. Since the odd mode requires flow across a "diameter" (see Fig. 2) and there is no preferred orientation in the actual cylindrical geometry, one would expect the onset of instability as a growing perturbation to break up the flow.

The curves of neutral stability are given in Fig. 3 for molten iron and also mercury. Points on each curve (representing a given value of $b'$) were computed at $\mathbf{K} = 0{\cdot}0625$, 0·125, 0·25, 0·5, 1·0, 2·0, 4·0, 8·0 and 16·0. No solutions were found for $\mathbf{K} \geqslant 4{\cdot}0$ nor for any value of $\mathbf{K}$ along $b' = 100$. For each value of $b'$ the critical Grashof number corresponds to a space period or wavelength of one radius, i.e. $\mathbf{K} = 1$. The critical values are plotted against $b'$ in Fig. 4.

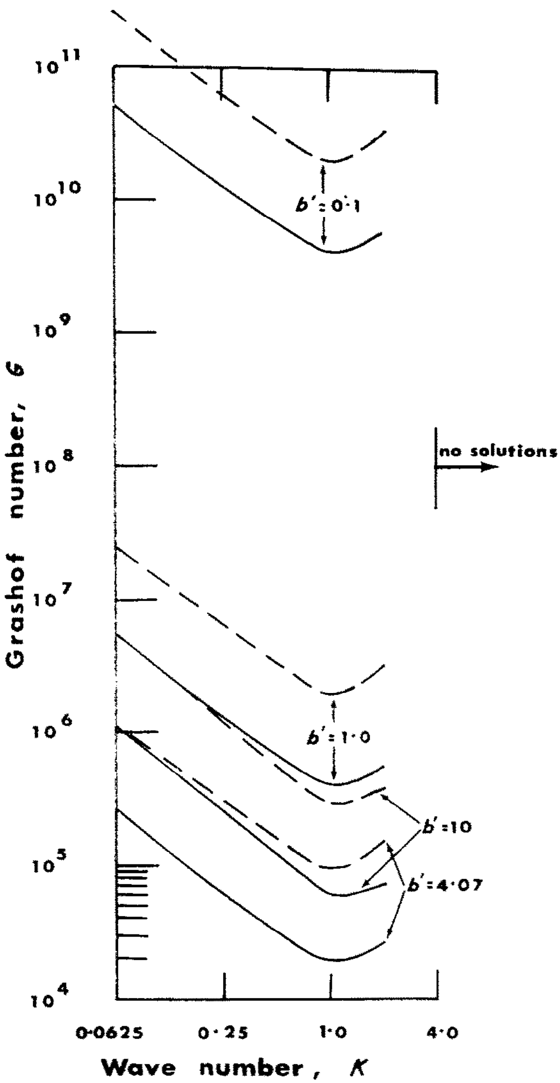


FIG. 3. Neutral stability curves for odd mode: —— molten iron ($P_r = 0{\cdot}1$); — — mercury ($P_r = 0{\cdot}02$).

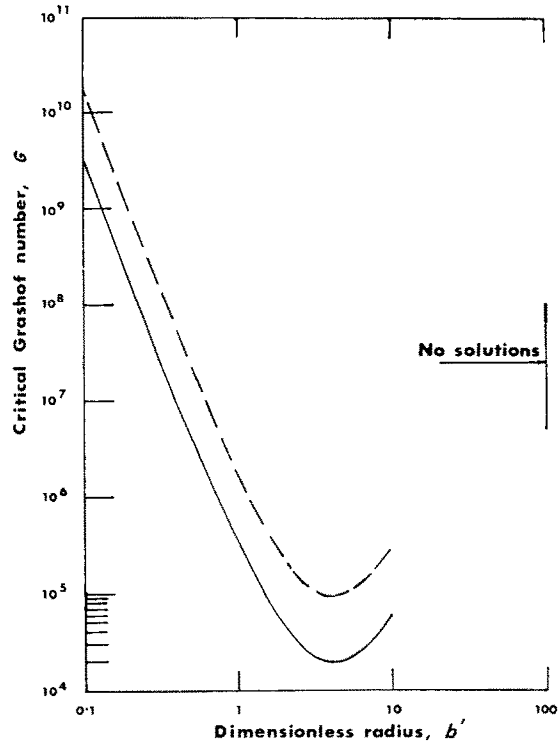


FIG. 4. Critical Grashof number vs $b'$: —— molten iron ($P_r = 0{\cdot}1$); — — mercury ($P_r = 0{\cdot}02$).

For a given exciting current it is seen that instability is most apt to set in at the frequency corresponding to maximum velocity or when $b' = 4{\cdot}07$. The minimum critical Grashof number, $G_m$, is 19 000 for molten iron and 95 000 for mercury.

By way of comparison the critical Rayleigh number (equal to $P_r\, G_m$) for the onset of thermal convection in the Bénard problem is 1708 when both surfaces are rigid and 1101 when the upper surface is free [10]. The corresponding values of $G_m$ for molten iron are 17 080 and 11 010 and are to be compared with a value of 19 100 for this analysis.

The value of the dimensionless frequency corresponding to $b' = 4{\cdot}07$ and $G_m$ that was calculated for molten iron is $\boldsymbol{\Omega} = 138{\cdot}6$. This corresponds to a perturbation frequency of $0{\cdot}504 \times 10^{-4}$ c/s and is consistent with the earlier assumption that $\omega \ll \omega_0$.

Lastly, it is of interest to calculate the maximum temperature difference $Q_1$ which cannot be exceeded if the flow is to remain stable. From the definition of the Grashof number, $Q_1$ is given by

$$Q_1 = G\nu^2/\beta g b^3$$

and is proportional to $G$ and inversely proportional to the "radius" cubed. At $b' = 4{\cdot}07$ and a charge of molten iron excited at 60 c/s the radius is $b = 0{\cdot}156$ m and $Q_1 = 0{\cdot}0012$°C. However, at a frequency of 960 c/s and $b' = 4{\cdot}07$, $Q_1$ increases by a factor of $4^3$ to a value of $0{\cdot}08$°C. These calculations illustrate that except for very small furnaces and/or very high values of $b'$ the tolerable temperature gradient is small, and the stirring action under the influence of thermal buoyancy forces is turbulent.

## REFERENCES

1. N. J. Damaskos, F. J. Young and W. F. Hughes, The magnetohydrodynamics of the coreless induction furnace, *Proc. Inst. Electron. Engrs* **110**, 1089–1095 (1963).
2. G. Z. Gershuni and E. M. Zhukhovitskii, Stability of the stationary convective flow of an electrically conducting liquid between parallel vertical plates in a magnetic field, *Zh. Eksper. Teor. Fiz.* **34**, 465–470 (1958).
3. S. Chandrasekhar, *Hydrodynamic and Hydromagnetic Stability*, Chapter 2. Clarendon Press, Oxford (1961).
4. O. M. Rayleigh, On convection currents in a horizontal layer of fluid, when the higher temperature is on the under side, *Phil. Mag.* **32**, 529–546 (1916).
5. S. H. Crandall, *Engineering Analysis*, pp. 147–154. McGraw-Hill, New York (1956).
6. L. Collatz, *The Numerical Treatment of Differential Equations*, pp. 28–33. Springer-Verlag, Berlin (1959).
7. W. J. Duncan, The principles of the Galerkin method, Aero. Res. Comm. Rept. and Mem. 1848, pp. 589–612 (1938).
8. L. V. Kantorovich and V. I. Krylov, *Approximate Methods of Higher Analysis*, pp. 258–304. Interscience Publishers, Groningen (1958).
9. J. T. Stuart, On the stability of viscous flow between parallel planes in the presence of a co-planar magnatic field, *Proc. Roy. Soc.* **A221**, 189–206 (1954).
10. A. Pellew and R. V. Southwell, On maintained convective motion in a fluid heated from below, *Proc. Roy. Soc.* **A176**, 312–343 (1940).
11. P. Grandjean, Contribution à l'étude du brassage electromagnétique dans un bain métallique en fusion, Thesis. University of Paris (1946).

**Résumé**—La stabilité de l'écoulement laminaire permanent d'un fourneau à induction idéalisé qui a été décrit auparavant est analysée au moyen de la technique des perturbations employée ordinairement pour les analyses de la stabilité [1]. On montre que le nombre de Grashof critique minimal pour le fer fondu est 19 000 pour un rapport de profondeur d'effet de peau au rayon de un demi. Les calculs montrent alors que le gradient de température tolérable le long du rayon est très petit telle façon que l'agitation sous l'action des forces d'Archimède thermiques est généralement turbulente.

**Zusammenfassung**—Mit Hilfe einer gewöhnlich für Stabilitätsanalysen verwendeten Störtechnik, wird die Stabilität der vorher abgeleiteten stationären laminaren Strömung eines idealisierten Induktionsofens analysiert [1]. Es wird gezeigt, dass die kleinste kritische Grashofzahl für geschmolzenes Eisen 19 000 ist, die bei einer Wandstärke entsprechend einem Radienverhältnis $\frac{1}{2}$ auftritt. Die Berechnung zeigt dann, dass der zulässige Temperaturgradient am Radius sehr klein ist, sodass die Rührwirkung unter dem Einfluss thermischer Auftriebskräfte im allgemeinen turbulent ist.

**Аннотация**—Устоичивость стационарного ламинарного потока в идеальной индукционной печи анализируется с помощью метода возмущений, обычно используемого для анализа устойчивости [1]. Показано, что минимальное критическое число Грасгофа для расплавленного железа составляет 19000 при отношении эффективной глубины проникновения переменного тока к радиусу 1 : 2. Расчетом показано, что допустимый температурный градиент поперек радиуса очень мал, так что перемешивание под влиянием термических подъемных сил является турбулентным.